EPJ Web of Conferences **175**, 05022 (2018) https://doi.org/10.1051/epjconf/201817505022
Lattice 2017

$\pi\pi$ P-wave resonant scattering from lattice QCD

Srijit Paul[1,6,⋆], *Constantia* Alexandrou[2,1], *Luka* Leskovec[3], *Stefan* Meinel[3,4], *John W.* Negele[5], *Marcus* Petschlies[7], *Andrew* Pochinsky[5], *Jesus Gumaro* Rendon Suzuki[3], and *Sergey* Syritsyn[8]

[1] *Computation-based Science and Technology Research Center, The Cyprus Institute, 20 Kavafi Str., Nicosia, 2121, Cyprus*
[2] *Department of Physics, University of Cyprus, POB 20537, 1678 Nicosia, Cyprus*
[3] *Department of Physics, University of Arizona, Tucson, AZ 85721, USA*
[4] *RIKEN BNL Research Center, Brookhaven National Laboratory, Upton, NY 11973, USA*
[5] *Center for Theoretical Physics, Massachusetts Institute of Technology, Cambridge, MA 02139, USA*
[6] *Department of Mathematics and Natural Sciences, University of Wuppertal, D-42119 Wuppertal, Germany*
[7] *Helmholtz-Institut für Strahlen- und Kernphysik, University of Bonn, D-53115 Bonn, Germany*
[8] *Department of Physics and Astronomy, Stony Brook University, Stony Brook, NY 11794, USA*

Abstract. We present a high-statistics analysis of the ρ resonance in $\pi\pi$ scattering, using $2+1$ flavors of clover fermions at a pion mass of approximately 320 MeV and a lattice size of approximately 3.6 fm. The computation of the two-point functions are carried out using combinations of forward, sequential, and stochastic propagators. For the extraction of the ρ-resonance parameters, we compare different fit methods and demonstrate their consistency. For the $\pi\pi$ scattering phase shift, we consider different Breit-Wigner parametrizations and also investigate possible nonresonant contributions. We find that the minimal Breit-Wigner model is sufficient to describe our data, and obtain $am_\rho = 0.4609(16)_{stat}(14)_{sys}$ and $g_{\rho\pi\pi} = 5.69(13)_{stat}(16)_{sys}$. In our comparison with other lattice QCD results, we consider the dimensionless ratios am_ρ/am_N and am_π/am_N to avoid scale setting ambiguities.

1 Introduction

The simplest QCD-unstable hadron is the ρ resonance, which decays into two pions with a branching ratio of 99.9%. As such, it is considered a benchmark for hadron spectroscopy on the lattice.

The ρ resonance appears as a pole in the $I = 1$ elastic P-wave $\pi\pi$ scattering amplitude. Because the scattering is elastic, the energy dependence of the scattering amplitude can be expressed in terms of a single real number, the phase shift. For a simple resonance, such as the ρ, the phase shift starts near 0 at the threshold, then goes through $\pi/2$ when the invariant mass is near the mass of the resonance, and continues toward π as the invariant mass leaves the resonance region.

While the Maiani-Testa theorem [1] prohibits the extraction of scattering amplitudes directly from Euclidean correlation functions in infinite volume (except at the threshold), Lüscher's method [2] circumvents the basic assumptions of this theorem and takes advantage of the finite lattice volume.

⋆ Speaker, e-mail: s.paul@hpc.leap.eu

The Lüscher quantization condition provides a (many-to-one) mapping between the discrete finite-volume multi-hadron spectrum and the elastic scattering amplitude. The relation was initially derived in the rest frame, and was extended to moving frames and coupled channels in Refs. [3–9].

Here, we present a high-statistics lattice QCD calculation of $I = 1$ P-wave $\pi\pi$ scattering, using 2+1 flavors of clover fermions at a pion mass of approximately 320 MeV and a lattice size of approximately 3.6 fm [10]. At each stage of the analysis, we compare different fit methods and demonstrate their consistency. We explore different parametrizations for the energy dependence of the scattering phase shift, and investigate whether a nonresonant background contribution is present.

2 Lattice methods and parameters

We use an ensemble of 1041 gauge-field configurations with $N_f = 2 + 1$ clover-improved Wilson fermions on a large $32^3 \times 96$ lattice with $a \approx 0.114$ fm. The pion mass is $m_\pi \approx 320$ MeV, and the strange-quark mass is consistent with its physical value as determined by the "η_s" mass.

To extract the energy spectrum in the $I = 1$, $J^P = 1^-$ channel, we use two types of interpolating operators: i) single-hadron operators $\bar{d}\Gamma u$, where $\Gamma \in \{\gamma_i, \gamma_0\gamma_i\}$, and ii) two-hadron operators of the form $(\pi^+\pi^0 - \pi^0\pi^+)/\sqrt{2}$, where $\pi^+ = \bar{d}\gamma_5 u$ and $\pi^0 = (\bar{u}\gamma_5 u - \bar{d}\gamma_5 d)/\sqrt{2}$ are individually projected to specific momenta. We build (3×3) or (4×4) two-point correlation matrices $C_{ij}(t) = \langle O_i(t) O_j^\dagger(0)\rangle$. The Wick contractions, shown in Fig. 1, are implemented using combinations of forward, sequential, and stochastic propagators. Compared to the distillation approach [11], our method has the advantage that the computational cost is independent of the chosen smearing width and scales linearly with the lattice volume. To map out the energy dependence of the $\pi\pi$ scattering amplitude, we use several moving frames with total momenta $\vec{P}$ and irreducible representations as listed in Table 1.

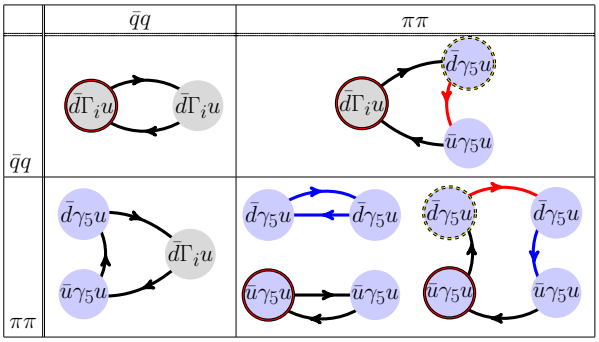

Figure 1. Wick contractions for the two-point correlation matrix. The source location for the forward propagator is shown with a black circle around the interpolating field, while a dotted circle indicates a sequential source. The red lines indicate sequential propagators and the blue lines indicate stochastic all-to-all propagators. The lower left diagram is not computed directly, and is instead obtained as the conjugate of the upper right diagram.

3 Spectrum results

To determine the energy levels E_n from the two-point correlation matrices C_{ij}, we compare three different fit methods and carefully study the dependence on the fit ranges. In the first two methods, we fit the principal correlators $\lambda_n(t, t_0)$ obtained from the generalized eigenvalue problem

$\vec{P}\,[\frac{2\pi}{L}]$	Little group	Irrep Λ
$(0,0,0)$	O_h	T_1^-
$(0,0,1)$	D_{4h}	A_2^-, E
$(0,1,1)$	D_{2h}	B_1^-, B_2^-, B_3^-
$(1,1,1)$	D_{3d}	A_2^-, E^-

Table 1. Moving frames and corresponding symmetry groups and irreducible representations.

$C_{ij}(t)\ u_j^n = \lambda_n(t,t_0)\ C_{ij}(t_0)\ u_j^n$, using either the single-exponential function $\lambda^n(t,t_0) = e^{-E_n(t-t_0)}$ or a two-exponential function $\lambda^n(t,t_0) = (1-B)\ e^{-E_n(t-t_0)} + B\ e^{-E'_n(t-t_0)}$. In our third method, we directly fit the correlation matrix (or a submatrix thereof) using the multi-exponential form $C_{ij}(t) = \sum_{n=1}^{N_{states}} Z_{i,n}\ Z_{j,n}\ e^{-E_n t}$, with N_{states} equal to the dimension of the matrix. As shown in Fig. 2, the different methods give consistent results. After choosing the nominal fit result, we estimate the remaining systematic uncertainty by varying $t_{\min}$.

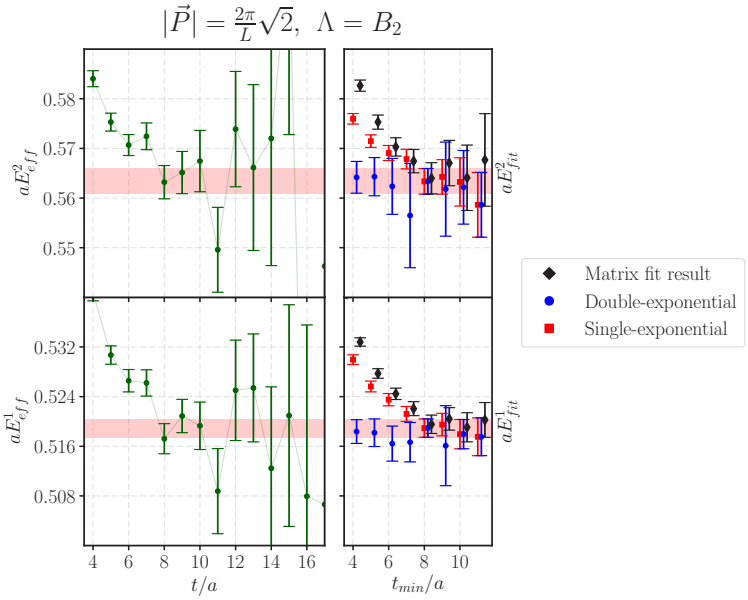

Figure 2. Spectrum results in the momentum frame $\frac{L}{2\pi}|\vec{P}| = \sqrt{2}$ and irrep $\Lambda = B_2$. The green data points on the left panel correspond to the effective energies of the GEVP principal correlators, $aE^n_{eff}(t) = \ln \frac{\lambda_n(t,t_0)}{\lambda_n(t+a,t_0)}$. In the right panel we present the fitted energies as a function of t_{min}/a. The extracted energies, indicated with the bands, are taken from the single-exponential principal-correlator fits with $t_{\min}/a = 8$.

4 Extraction of resonant parameters using the Lüscher method

The discrete multi-hadron spectrum in the finite volume is related to the infinite-volume elastic scattering phase shifts δ_ℓ via the quantization condition first derived by Lüscher [2] and recently reviewed

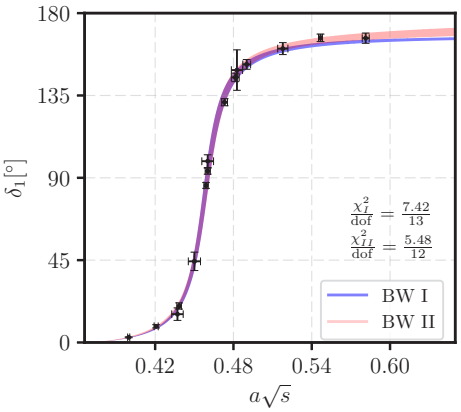

Figure 3. Fits of the purely resonant Breit-Wigner models, without (**BW I**) and with (**BW II**) Blatt-Weisskopf barrier factors, to the phase shift data points.

Fit type	χ^2/dof	am_ρ	$g_{\rho\pi\pi}$	$(ar_0)^2$
BW I Fit to δ_1	0.571	0.4599(19)(13)	5.76(16)(12)	
BW I t-matrix fit	0.374	0.4609(16)(14)	5.69(13)(16)	
BW II Fit to δ_1	0.457	0.4600(18)(13)	5.79(16)(12)	8.6(8.0)(1.2)
BW II t-matrix fit	0.318	0.4603(16)(14)	5.77(13)(13)	9.6(5.9)(3.7)

Table 2. Fit results for the Breit-Wigner models I and II, obtained either by first extracting individual phase shift points and then fitting the model to the points ("Fit to δ_1"), or by directly fitting the model to the whole energy spectrum ("t-matrix fit").

in Ref. [12]:

$$\det\Big(\mathbb{1} + it_\ell(s)(\mathbb{1} + i\mathcal{M}^{\vec{P}})\Big) = 0. \tag{1}$$

Above, $t_\ell(s) = \frac{1}{\cot\delta_\ell(s) - i}$ is the ℓ-wave scattering amplitude and $\mathcal{M}^{\vec{P}}$ is a matrix-valued function that depends on the spectrum and volume. The quantization condition can be simplified for each momentum frame according to the symmetries in that frame. The resulting equations for the cases listed in Table 1 are given in Ref. [10].

The numerical analysis can be performed in two different ways: i) mapping each individual energy level to a single phase-shift point, and then performing a secondary fit of a model for $\delta(s)$, and ii) directly fitting the parameters of the model to the whole energy spectrum ("t-matrix fit"). We confirmed that both approaches give the same results.

We first considered purely resonant Breit-Wigner-parametrizations for the phase shift:

$$\delta^{BW}(s) = \cot^{-1}\frac{m_R^2 - s}{\sqrt{s}\,\Gamma(s)}, \tag{2}$$

with two different models for Γ:

- **BW I:** This is the simplest form determined by the phase space for a P-wave decay:

$$\Gamma_I(s) = \frac{g^2_{\rho\pi\pi}}{6\pi}\frac{k^3}{s}, \tag{3}$$

where $g_{\rho\pi\pi}$ is the resonance coupling and k is the scattering momentum, $2\sqrt{m_\pi^2 + k^2} = \sqrt{s}$.

- **BW II:** The above P-wave decay width modified with Blatt-Weisskopf barrier factors [13]:

$$\Gamma_{II}(s) = \frac{g^2_{\rho\pi\pi}}{6\pi}\frac{k^3}{s}\frac{1+(k_R r_0)^2}{1+(k r_0)^2}, \tag{4}$$

where k_R is the scattering momentum at the resonance position and r_0 is the radius of the centrifugal barrier.

The two models are compared in Fig. 3, where we can see that both models describe the data points well. The fitted parameters are presented in Table 2. We find that the centrifugal barrier radius r_0 is not statistically significant. Additionally, the other parameters are consistent between the two models.

The $\pi\pi$ scattering amplitude could in principle also contain a contribution from a non-resonant (NR) background phase. Phenomenologically, this contribution would correspond to the two pions scattering without any resonances being created. We therefore continue the analysis by adding three different background phase models to the resonant phase shift model **BW I**, writing $\delta(s) = \delta^{BW}(s) + \delta^{NR}(s)$, with

- **NR I:** a constant nonresonant phase A,

$$\delta^{NR}_I(s) = A. \tag{5}$$

- **NR II:** a nonresonant phase depending linearly on s,

$$\delta^{NR}_{II}(s) = A + Bs. \tag{6}$$

- **NR III:** zeroth order nonresonant effective-range expansion (ERE),

$$\delta^{NR}_{III}(s) = \operatorname{arccot}\frac{2a_1^{-1}}{\sqrt{s - s^{thres}}}, \tag{7}$$

where a_1^{-1} is the inverse scattering length and $s^{thres} = 4m_\pi^2$ is the $\pi\pi$ threshold invariant mass.

The fits of $\delta(s) = \delta^{BW}(s) + \delta^{NR}(s)$ are shown in Fig. 4 and give the parameters listed in Table 3. We find that the nonresonant contributions are statistically consistent with zero. We therefore quote the results of the t-matrix fit to the pure **BW I** model, $am_\rho = 0.4609(16)(14)$ and $g_{\rho\pi\pi} = 5.69(13)(16)$, as our final parameters.

5 Comparison to other studies

In Fig. 5, we compare our results for $g_{\rho\pi\pi}$ and m_ρ with those from previous lattice studies. We use both the values of m_π and m_ρ in physical units as reported in each lattice QCD study and dimensionless ratios $\frac{am_\pi}{am_N}$ and $\frac{am_\rho}{am_N}$ to avoid systematic errors in setting the scale. Our calculation gives

$$\begin{aligned}\frac{am_\pi}{am_N} &= 0.2968(13),\\ \frac{am_\rho}{am_N} &= 0.7476(38).\end{aligned} \tag{8}$$

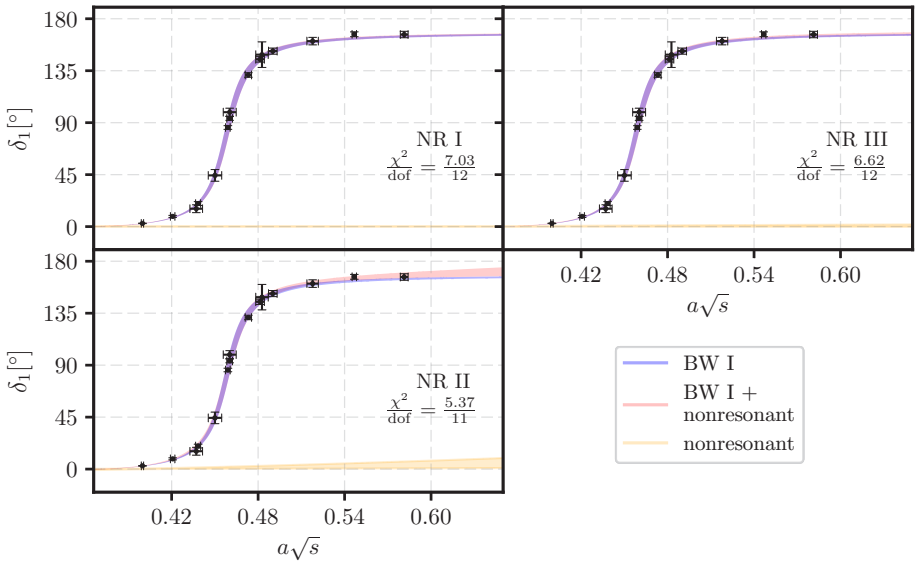

Figure 4. Fits of $\delta(s) = \delta^{BW}(s) + \delta^{NR}(s)$, where $\delta^{BW}(s)$ is the minimal Breit-Wigner model **BW I** and $\delta^{NR}(s)$ is one of the three different nonresonant models.

Model	χ^2/dof	am_ρ	$g_{\rho\pi\pi}$		
NR I	0.586	0.4600(19)(13)	5.74(17)(14)	$A = 0.16(31)(18)°$	
NR II	0.488	0.4602(19)(13)	5.84(21)(20)	$A = -2.9(2.7)(3.4)°$	$a^{-2}B = 19.2(16.6)(20.1)°$
NR III	0.552	0.4601(19)(13)	5.74(16)(13)	$aa_1^{-1} = -19.8(27.4)(98.1)$	

Table 3. Fit results for the phase shift model combining the resonant Breit-Wigner model **BW I** with the nonresonant models **NR I-III**.

Our result for the coupling $g_{\rho\pi\pi}$ is in good agreement with previous studies, both as a function of m_π and am_π/am_N. For the ratio am_ρ/am_N, the more recent $N_f = 2 + 1$ results obtained with clover fermions appear to approach the physical point quite linearly as a function of am_π/am_N. Extrapolations of the lattice data to the physical point using unitarized chiral perturbation theory were discussed in Refs. [14] and [15].

6 Conclusions

A precision lattice QCD study of isospin-1, P-wave $\pi\pi$ scattering with the Lüscher method is presented using a lattice of size $(3.6\,\mathrm{fm})^3 \times (10.9\,\mathrm{fm})$ at a pion mass of approximately 320 MeV. The large volume, in combination with several moving frames, allows us to thoroughly map out the scattering phase shift near the ρ resonance. We find that the amplitude is well described by the simplest Breit-Wigner model without any modifications or additions of a nonresonant background phase. In comparing the results of different lattice calculations for m_ρ, a more consistent picture emerges when the dimensionless ratio am_ρ/am_N is considered as a function of am_π/am_N.

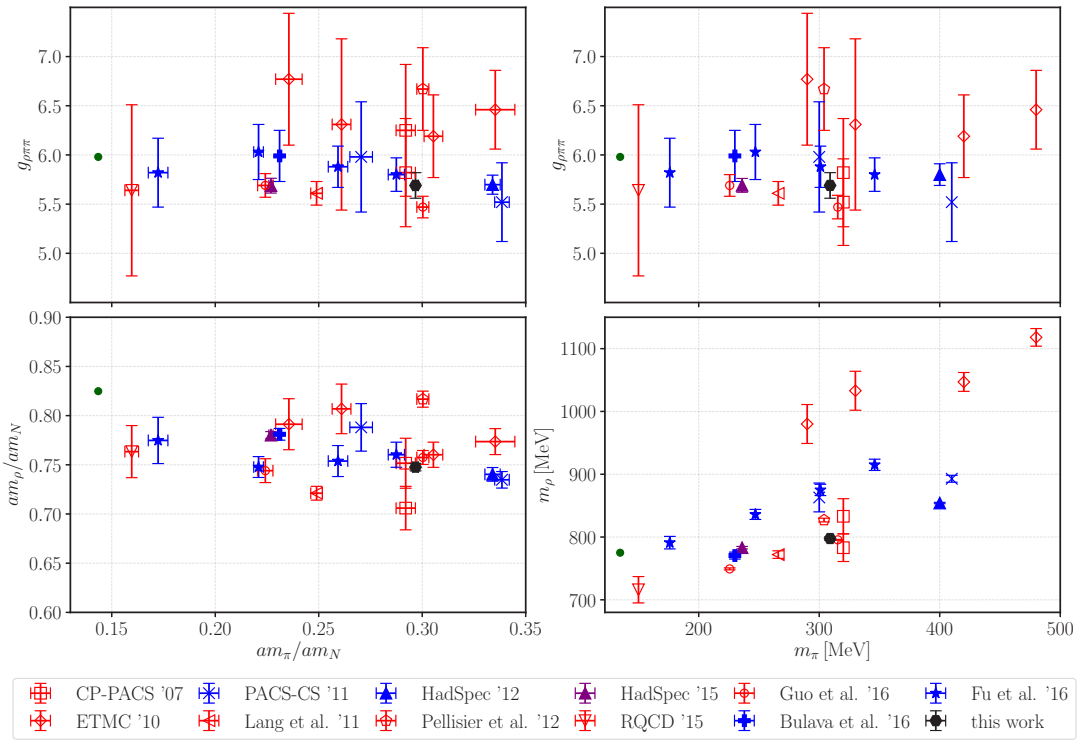

Figure 5. Comparison of our results for $g_{\rho\pi\pi}$ and m_ρ (plotted with black hexagons) with those reported by the CP-PACS collaboration (CP-PACS '07) [16], the ETMC collaboration (ETMC '10) [17], the PACS-CS collaboration (PACS-CS '11) [18], Lang et al. (Lang et al. '11) [19], the Hadron Spectrum collaboration (HadSpec '12 and HadSpec '15) [20, 21], Pellisier et al. (Pellisier et al. '12) [22], the RQCD collaboration (RQCD '15) [23], Guo et al. (Guo et al. '16) [24], Bulava et al. (Bulava et al. '16) [25], and Fu et al. (Fu et al. '16) [26]. The $N_f = 2$ results are plotted in red, the $N_f = 2 + 1$ results are plotted in blue, and the $N_f = 2 + 1$ calculation that explicitly included the $K\bar{K}$ channel is plotted in purple. The green circles show the experimental values.

Acknowledgements

We thank Kostas Orginos for providing the gauge ensemble, which was generated with XSEDE resources supported by NSF grant number ACI-1053575. Our calculations were performed at NERSC, supported by the U.S. DOE under Contract No. DE-AC02-05CH11231. SM and GR are supported by NSF award number 1520996. SM and SS also thank the RIKEN BNL Research Center for support. JN was supported in part by the DOE Office of Nuclear Physics under grant DE-SC-0011090. AP was supported in part by the U.S. Department of Energy Office of Nuclear Physics under grant DE-FC02-06ER41444. S.P. is supported by the Horizon 2020 of the European Commission research and innovation programme under the Marie Sklodowska-Curie grant agreement No. 642069. We acknowledge the use of the USQCD software QLUA[27] and the underlying libraries.

References

[1] L. Maiani, M. Testa, Phys. Lett. **B245**, 585 (1990)

[2] M. Lüscher, Nucl. Phys. **B354**, 531 (1991)
[3] K. Rummukainen, S.A. Gottlieb, Nucl. Phys. **B450**, 397 (1995), hep-lat/9503028
[4] C.H. Kim, C.T. Sachrajda, S.R. Sharpe, Nucl. Phys. **B727**, 218 (2005), hep-lat/0507006
[5] N.H. Christ, C. Kim, T. Yamazaki, Phys. Rev. **D72**, 114506 (2005), hep-lat/0507009
[6] L. Leskovec, S. Prelovsek, Phys. Rev. **D85**, 114507 (2012), 1202.2145
[7] M.T. Hansen, S.R. Sharpe, Phys. Rev. **D86**, 016007 (2012), 1204.0826
[8] M. Göckeler, R. Horsley, M. Lage, U.G. Meissner, P.E.L. Rakow, A. Rusetsky, G. Schierholz, J.M. Zanotti, Phys. Rev. **D86**, 094513 (2012), 1206.4141
[9] R.A. Briceño, Phys. Rev. **D89**, 074507 (2014), 1401.3312
[10] C. Alexandrou, L. Leskovec, S. Meinel, J. Negele, S. Paul, M. Petschlies, A. Pochinsky, G. Rendon, S. Syritsyn, Phys. Rev. **D96**, 034525 (2017), 1704.05439
[11] M. Peardon, J. Bulava, J. Foley, C. Morningstar, J. Dudek, R.G. Edwards, B. Joo, H.W. Lin, D.G. Richards, K.J. Juge (Hadron Spectrum), Phys. Rev. **D80**, 054506 (2009), 0905.2160
[12] R.A. Briceno, J.J. Dudek, R.D. Young (2017), 1706.06223
[13] F. Von Hippel, C. Quigg, Phys. Rev. **D5**, 624 (1972)
[14] B. Hu, R. Molina, M. Döring, M. Mai, A. Alexandru (2017), 1704.06248v1
[15] P.C. Bruns, M. Mai (2017), 1707.08983
[16] S. Aoki et al. (CP-PACS), Phys. Rev. **D76**, 094506 (2007), 0708.3705
[17] X. Feng, K. Jansen, D.B. Renner, Phys. Rev. **D83**, 094505 (2011), 1011.5288
[18] S. Aoki et al. (PACS-CS), Phys. Rev. **D84**, 094505 (2011), 1106.5365
[19] C.B. Lang, D. Mohler, S. Prelovsek, M. Vidmar, Phys. Rev. **D84**, 054503 (2011), [Erratum: Phys. Rev.D89,no.5,059903(2014)], 1105.5636
[20] J.J. Dudek, R.G. Edwards, C.E. Thomas (Hadron Spectrum), Phys. Rev. **D87**, 034505 (2013), [Erratum: Phys. Rev. D90, no.9, 099902 (2014)], 1212.0830
[21] D.J. Wilson, R.A. Briceño, J.J. Dudek, R.G. Edwards, C.E. Thomas, Phys. Rev. **D92**, 094502 (2015), 1507.02599
[22] C. Pelissier, A. Alexandru, Phys. Rev. **D87**, 014503 (2013), 1211.0092
[23] G.S. Bali, S. Collins, A. Cox, G. Donald, M. Göckeler, C.B. Lang, A. Schäfer (RQCD), Phys. Rev. **D93**, 054509 (2016), 1512.08678
[24] D. Guo, A. Alexandru, R. Molina, M. Döring, Phys. Rev. **D94**, 034501 (2016), 1605.03993
[25] J. Bulava, B. Fahy, B. Hörz, K.J. Juge, C. Morningstar, C.H. Wong, Nucl. Phys. **B910**, 842 (2016), 1604.05593
[26] Z. Fu, L. Wang, Phys. Rev. **D94**, 034505 (2016), 1608.07478
[27] *USQCD software Qlua package*, https://usqcd.lns.mit.edu/w/index.php/QLUA